Noble gases in carbonatites of Sung Valley and Ambadongar: Implications for trapped components

S. Basu [1], S.V.S. Murty [*]

Planetary and Geosciences Division, Physical Research Laboratory, Ahmedabad 380009, India

Abstract

Carbonates, apatites and magnetites from Sung Valley (107 Ma) and carbonates from Ambadongar (65 Ma), two carbonatitic complexes of India, have been analysed for noble gases by vacuum crushing and pyrolysis (apatites only). During vacuum crushing $^{20}Ne/^{22}Ne$ and $^{129}Xe/^{132}Xe$ of up to 12.1 and 1.06 respectively in Sung Valley and up to 10.3 and 1.06 respectively in Ambadongar have been measured. This clearly indicates presence of mantle noble gases. The $^{3}He/^{4}He$ are up to $\approx 9.01 \pm 0.85$ R_A for Sung Valley magnetites (where R_A is the atmospheric $^{3}He/^{4}He$ of 1.4×10^{-6}). The $^{21}Ne/^{22}Ne$ lie in the range of 0.031 to 0.069 for Sung Valley and 0.030 to 0.054 for Ambadongar. This is consistent with the presence of a MORB component admixed with crustal noble gases introduced into the lithospheric mantle during subduction. However, the crustal signatures are differently manifested in the carbonates and the late crystallising magnetites from Sung Valley owing to the relative variation of He/Ne ratios between the residual degassed magma (derived from the MORB source) and the vapour phase. As the relative He/Ne ratio of the magma increases progressively, assimilation of the crustal component from the lithosphere strongly affects the Ne, but not the He isotopic composition of the late crystallising magnetites. Ar and Xe compositions are also consistent with MORB contribution. Some dilution of magmatic signatures is clearly observed in the late stage ferrocarbonatites from Ambadongar and magnetites from Sung Valley, probably the effect of hydrothermal fluids bearing atmospheric gases.

Unlike the Kola carbonatites which was dominated by plume component, both Sung Valley and Ambadongar have been generated during the waning stages of plume magmatism leading to dilution and replacement of plume signatures by increasing input from MORB and lithospheric components as the uprising plume induces their melting and subsequent entrainment.
© 2006 Elsevier B.V. All rights reserved.

Keywords: Carbonatites; MORBs; Lithosphere; Hydrothermal fluids; Plume component; Noble gases

1. Introduction

The origin of carbonatites from the mantle is well established although no unique source region can be ascribed to them (Barker, 1989). Carbonatites have been reported from both depleted and enriched mantle from Sr, Nd and Pb isotopic compositions (Bell and Blekinshop, 1987; Kwon et al., 1989; Simonetti et al., 1998). The isotopic composition of $^{20}Ne/^{22}Ne \sim 12.5$ (Trieloff et al., 2000) [although values ≥ 13.0 have also been reported (Yokochi and Marty, 2004)] in mantle rocks is distinct from that of the atmosphere (9.8). $^{129}Xe/^{130}Xe$ ratios of between ~ 7.0 and 8.6 reported from mid-oceanic ridge basalts (MORBs), diamonds and

---

* Corresponding author. Tel.: +91 79 26314358; fax: +91 79 26301502.

E-mail addresses: sudeshnabg@yahoo.com (S. Basu), murty@prl.res.in (S.V.S. Murty).

[1] Present address: Isotope Geosciences Unit, Scottish Universities Environmental Research Centre, East Kilbride G75 0QF, UK.

carbonatites is also distinct from the atmosphere value (6.496) (Allègre et al., 1983; Staudacher et al., 1989; Sasada et al., 1997). Other noble gas isotopic ratios, in particular $^3He/^4He$, $^{21}Ne/^{22}Ne$ and $^{40}Ar/^{36}Ar$ are not only different for air and mantle but can also be used for distinguishing between degassed (MORB) and relatively undegassed plume (like Loihi) mantle sources (Trieloff et al., 2000, 2003; Stuart et al., 2003). Because of the low temperature ($\sim 600–770$ °C), (Secher and Larson, 1980), viscosity and density of carbonatitic melts, they are rapidly transported through the crust ensuring that they remain unaffected by crustal contamination (Bell, 2002).

The paucity of noble gas data from carbonatites is in part due to the difficulty in finding unaltered carbonatites that retain their magmatic signatures. The low noble gas concentration leaves them prone to overprinting by atmospheric contamination. Noble gas studies from the active extrusive carbonatitic volcano Oldoinyo Lengai, Tanzania, show a $^3He/^4He$ of 7.6 R_A and $^{40}Ar/^{36}Ar$ value of ~ 335 (Javoy et al., 1989). The only carbonatite to be extensively studied for noble gases is the Devonian Kola carbonatite from Russia. The studies indicate a plume source with $^{40}Ar/^{36}Ar$ of ~ 4000, $^{21}Ne/^{22}Ne$ of ~ 0.045 and $^3He/^4He$ of ~ 24 R_A (Marty et al., 1998; Tolstikhin et al., 2002). A similar, deep mantle source has also been advocated for Brazilian and Canadian carbonatites on the basis of $^{40}Ar/^{36}Ar \sim 6400$ and excess ^{129}Xe (Sasada et al., 1997). $^3He/^4He$ ratios up to ~ 14 R_A from the carbonatitic and alkali rock complexes of Mundwara and Sarnu, India is also indicative of a deep source (Basu et al., 1994). The present contribution discusses the results obtained from the first ever noble gas isotope analyses of carbonatites from Sung Valley and Ambadongar and their implications in an attempt to obtain insight into the origin of carbonatitic volcanism in general and the investigated complexes in particular.

2. Geological background and earlier studies

2.1. Sung Valley

The Sung Valley carbonatite complex consists of carbonatites and ultramafic–alkaline rocks and is associated with the major Um-Ngot lineament present in the Shillong Plateau (Fig. 1) (Krishnamurthy, 1988). The main rock type of the complex is pyroxenite into which carbonatites have been emplaced (Krishnamurthy, 1988). The major carbonatite type is calcitic with a few occurrences of dolomite-bearing calcite carbonatites. The Sung Valley carbonatites are believed to be related to the Kerguelen plume from their age (107.2 ± 0.8 Ma), the spatial proximity to the Sylhet traps, the HIMU-EM I signatures and Sr isotopic similarity to the Kerguelen basalts (Kent et al., 1992; Kumar et al., 1996; Ray et al., 1999; Kumar et al., 2003). The $\delta^{18}O$ values of these carbonatites fall in the mantle range implying no significant assimilation of ^{18}O-rich crustal material (Ray et al., 1999). Also the initial $^{87}Sr/^{86}Sr$ and $^{143}Nd/^{144}Nd$ of these rocks do not show any effect of crustal contamination (Veena et al., 1998). Nd, Pb and Sr isotopic systematics of Sung Valley suggests that these carbonatites were derived by partial melting of the sub-continental lithosphere
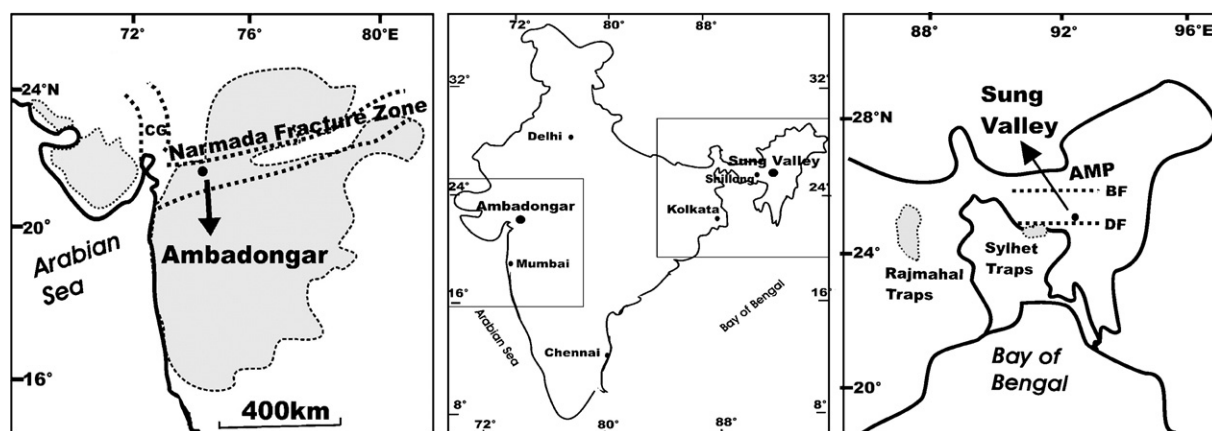

Fig. 1. Sketch map of India showing the approximate locations of the carbonatitic complexes of Ambadongar and Sung Valley. The shaded regions indicate the Deccan Traps (Ambadongar), and Rajmahal and Sylhet Traps (Sung Valley). The Ambadongar carbonatite is associated with the Narmada Fracture Zone as shown in the figure. Adjacent Cambay Graben (CG) is also shown in the figure. The Sung Valley carbonatitic complex is located in the Assam–Meghalaya–Plateau (AMP) bounded by the Brahmaputra Fault (BF) and the Dauki Fault (DF). (modified from Krishnamurthy, 1988; Ray et al., 1999, 2000).

metasomatized by fluids from mantle plumes (Veena et al., 1998).

2.2. Ambadongar

The sub-volcanic alkaline ring complex of Ambadongar consists of carbonatites, nephelinites and phonolites. It is located at the northern periphery of the Deccan flood basalts (Fig. 1) (Viladkar, 1981) and has been precisely dated to be 65.0 ± 0.3 Ma (Ray et al., 2000). Its spatial and temporal association with the Deccan basalts indicates an origin from the Reunion plume (Ray et al., 2000). The complex shows sequential emplacement of calcitic carbonatite, followed by dolomitic carbonatites and finally late-stage intrusions of ferro-carbonatites (Viladkar, 1981; Viladkar and Schidlowski, 2000). For the present study we have analysed carbonates from both calcitic (mono-mineralic) and ferro-carbonatites. On the basis of Sr, Nd and Pb isotopes, three distinct mantle components (Reunion plume, continental lithosphere and Indian MORB-like) have contributed to the magmatism (Simonetti et al., 1998). A very shallow level of emplacement is suggested for the Ambadongar carbonatites based on their sub-volcanic to volcanic association, extensive brecciation, late-stage carbonatitic veining and predominant feldspathic fenitization (Ray et al., 2000).

3. Experimental techniques

3.1. Sample characterisation

Samples have been collected from exposed transverse sections in road cuts using hand drills in Sung Valley and quarries in Ambadongar. Only fresh, unaltered samples have been selected. Calcite and dolomite formed in the early stages from carbonatitic magma are accompanied by silicates and oxides that react with water at low temperatures to form dolomite or ankerite, quartz, zeolite, fluorite, chlorite, rutile and haematite. Thin section studies have been carried out to distinguish between early and late stages of carbonatites and those showing late stage phases as well as recrystallization textures have been discarded (except the ferro carbonatites from Ambadongar). To confirm mineral identification X-ray diffraction (XRD) studies have been done on the carbonates and apatite. The carbonates and apatite have also been analysed for K, Na and Fe by atomic absorption spectroscopy (AAS) and Ca and Mg by Inductively-Coupled-Plasma-Atomic-Emission-Spectroscopy (ICPAES). Rare earth elements (REEs) and other trace elements

in apatites were analysed by Inductively-Coupled-Plasma-Mass-Spectrometry (ICPMS). Elemental analyses indicate that the carbonates separated from Sung Valley (SV-C1, SV-C2, SV-C3, SV-C4, and SV-C5) are calcitic in composition with up to 1.4% of Mg and 0.15% Fe. Carbonates evolve progressively showing a continuous transition from $Ca \rightarrow Mg \rightarrow Fe + Mg \rightarrow Mn + Fe$ from early to late stages (Hogarth, 1989) indicating that the Sung Valley carbonatites must have been generated during the early stages of carbonatitic magmatism. Care was taken to avoid collection of late-stage calcite veins. Apatite crystallization can also extend from early to late stages of carbonatitic magmatism. Most apatites have a La:Yb of $\sim 150-200:1$ but can be as low as 0.03:1 in secondary apatites (Hogarth, 1989). Earlier studies have revealed that apatites from the Kola carbonatites show an increase in HREEs from early to middle stages of development, along with progressive enrichment of Ba from ~ 0.04 to 0.19%, and Sr from 0.33 to 0.90% (Hogarth, 1989). The La/Yb (105), and low Ba, Sr concentrations (0.0018% and 0.17%) for the Sung Valley apatite (SV-A1) indicate that it was generated in the early stage of carbonatite magmatism. For Ambadongar, carbonates have been analysed from early-formed calcitic carbonatites (A-C1, A-C2, A-C6) and late stage ferro-carbonatites (A-C3, A-C4, A-C5).

3.2. Noble gas extraction procedures

Individual mm-sized grains of carbonates, apatites and magnetites were separated under optical microscope. Noble gases were extracted from apatite by both stepwise pyrolysis (P) and vacuum crushing (VC), while the carbonates and magnetites were only crushed. VC predominantly releases the trapped gases from the fluid inclusions with minimal contribution from the in-situ matrix-sited component. Also, it would be difficult to analyse the carbonates by P owing to the huge amount of CO_2 that would be released on their melting, difficult to handle by the getters. Subsequent to gas extraction by either technique, all noble gases were analysed following the procedure described in Murty (1997). For P, the apatite was wrapped in Al-foil and mounted in the sample line. The system was evacuated and baked up to ~ 150 °C overnight under high vacuum. Initially the sample was introduced into a double-walled quartz finger where it was combusted at 400 °C in presence of O_2 (at 2 Torr pressure) to remove surficial contaminants. It was then dropped into a Mo crucible and heated in steps up to 1800 °C to ensure complete release of gases.

Table 1
He, Ne, Ar and Xe abundances and isotopic ratios of all samples

No of strokes(VC) Or °C(P)	^{4}He (10^{-6})	^{22}Ne (10^{-10})	^{36}Ar (10^{-10})	^{132}Xe (10^{-12})	^{3}He/^{4}He (R/R_a)	^{21}Ne/^{22}Ne	^{20}Ne/^{22}Ne	^{40}Ar/^{36}Ar	^{129}Xe/^{132}Xe	^{4}He/^{21}Ne$_{corr}$[a] (10^7)
Sung Valley										
SV-C3(VC)(1.7g)										
50	17.3	0.3	2.6	1.8	3.95	0.0543	12.08	4395	1.05	
					±.35	±.0027	±.29	±40	±.01	
300	52.4	0.6	20.2	5.0	3.31	0.0477	11.64	3364	1.01	
					.29	.0026	.32	32	.01	
300	11.6	BL	2.5	1.4	2.46			3011	1.03	
					.43			27	.02	
Total	81.3	0.9	25.3	8.3	3.32	0.0495	11.78	3434	1.02	6.5
					.32	.0030	.44	33	.01	
SV-M3(VC) (1.5 g)										
15	17.7	0.2	2.9	BL	9.01	0.0492	10.05	1244		
					.85	.0031	.13	11		
500	44.2	0.2	4.3	BL	8.25	0.0657	10.27	1694		
					.70	.0048	.39	16		
500	11.4	BL	0.5	BL	8.41			2905		
					.71			21		
Total	73.4	0.4	7.7		8.46	0.0568	10.15	1591		6.0
					.77	.0033	.25	14		
SV-C1(VC)(2.0 g)										
15	3.4	0.4	6.9	2.8	3.74	0.0488	11.10	3432	1.03	
					.32	.0013	.16	32	.01	
300	9.3	0.6	13.4	8.5	2.57	0.0495	11.52	4956	1.05	
					.25	.0017	.28	46	.01	
300	1.2	0.2	1.8	BL	1.04	0.0489	11.38	4662		
					.48	.0038	.39	39		
Total	13.9	1.2	22.1	11.3	2.69	0.0489	11.36	4457	1.05	0.8
					.28	.0016	.25	41	.01	
SV-M1A(VC)(1.3 g)										
15	1.1	0.4	6.9	BL	7.60	0.0387	9.91	1199		
					.84	.0013	.22	11		
500	4.2	0.3	8.0	BL	6.95	0.0626	10.44	2193		
					.61	.0037	.33	45		
500	BL	BL	1.5	BL				1848		
								15		
Total	5.3	0.7	16.4		7.08	0.0475	10.11	1743		0.4
					.66	.0024	.26	28		
SV-M1B(VC)(1.5 g)										
15	0.9	0.3	4.2	BL	8.49	0.0489	10.20	900		
					.91	.0021	.09	8		
500	3.3	0.2	3.9	BL	7.86	0.0690	10.00	1761		
					.66	.0022	.14	16		
500	BL	BL	0.5	BL				2481		
								18		
Total	4.2	0.5	8.6		7.99	0.0576	10.11	1386		0.3
					.71	.0021	.11	13		
SV-C4(VC)(1.9 g)										
15	1.5	1.3	14.3	ND		0.0408	11.04	463		
						.0022	.51	5		
300	3.4	0.5	9.5	ND		0.0425	10.62	770		
						.0031	.57	7		
300	BL	BL	0.7	ND				1176		

Table 1 (*continued*)

No of strokes(VC) Or °C(P)	^{4}He (10^{-6})	^{22}Ne (10^{-10})	^{36}Ar (10^{-10})	^{132}Xe (10^{-12})	^{3}He/^{4}He (R/R_a)	^{21}Ne/^{22}Ne	^{20}Ne/^{22}Ne	^{40}Ar/^{36}Ar	^{129}Xe/^{132}Xe	^{4}He/^{21}Ne$_{corr}$[a] (10^7)
SV-C4(VC)(1.9 g)										
Total	4.9	1.8	24.5			0.0415 .0023	10.93 .53	10 604 6		0.3
SV-C5(VC)(1.5 g)										
15	1.2	5.7	7.3	1.5		0.0309 .0010	10.29 .03	496 5	0.98 .01	
300	2.9	0.5	6.4	2.0		0.0417 .0021	9.71 .18	847 8	0.99 .01	
300	BL	BL	0.1	BL				329 2		
Total	4.1	6.2	13.8	3.5		0.0318 .0010	10.25 .04	645 6	0.99 .01	0.5
SV-A1(VC)(470.7 mg)										
15	0.5	0.3	8.7	BL		0.0480 .0040	9.60 .22	2938 25		
500	4.3	0.4	6.6	BL		0.0544 .0055	5.79 .31	3843 32		
500	BL	BL	3.1	BL				1619 3		
Total	4.8	0.7	18.4			0.0515 .0050	7.58 .30	3040 24		0.2
SV-A1(P′)(87.3 mg)										
400	5.3	22.4	ND	ND		0.0365 .0012	9.92 .14			
1200	9.0	31.8	ND	ND		0.0458 .0009	11.06 .26			
1400	2.5	36.6	ND	ND		0.0559 .0012	4.71 .21			
1600	1.0	26.4	ND	ND		0.0443 .0010	10.47 .46			
Total	17.8	117.2				0.0468 .0011	8.73 .36			
SV-C2(VC)(1.5 g)										
15	ND	ND	6.3	1.6				2107 21	1.06 .01	
300	ND	ND	7.4	2.5				3832 38	0.99 .01	
300	ND	ND	1.9	0.6				3409 47	1.00 .01	
Total			15.6	4.7				3082 32	1.02 .01	
SV-A2(P)(113.0 mg)										
400	5.7	207	BL	BL		0.0313 .0010	9.78 .01			
600	8.1	184	13.6	BL		0.0300 .0019	9.66 .02	2022 135		
950	14.4	113	BL	BL		0.0297 .0123	8.75 .11			
1200	BL	BL	4.1	BL				402.0 .6		
1400	BL	BL	1.2	BL				332.0		

Table 1 (*continued*)

No of strokes(VC) Or °C(P)	^{4}He (10^{-6})	^{22}Ne (10^{-10})	^{36}Ar (10^{-10})	^{132}Xe (10^{-12})	^{3}He/^{4}He (R/R_a)	^{21}Ne/^{22}Ne	^{20}Ne/^{22}Ne	^{40}Ar/^{36}Ar	^{129}Xe/^{132}Xe	^{4}He/^{21}Ne$_{corr}$[a] (10^7)
SV-A2(P)(113.0 mg)								.6		
1700	BL	BL	0.8	BL				1692		
								16		
Total	28.2	503	19.7			0.0302	9.43	1567		0.2
						.0038	.04	94		
Ambadongar A-C1(VC)(755.8 mg)										
15	3.9	6.4	83.6	9.5		0.0333	10.09	5301	1.05	
						±.0010	±.03	±103	±.01	
300	5.9	6.1	81.2	12.4		0.0367	10.19	2770	1.05	
						.0011	.08	54	.02	
300	0.8	0.7	8.0	BL		0.0544	10.07	3537		
						.0021	.13	65		
Total	10.6	13.2	172.8	21.9		0.0355	10.14	4030	1.05	0.1
						.0010	.06	78	.02	
A-C2 (VC)(1.7 g)										
15	2.2	4.4	61.2	5.3		0.0321	10.04	1468	1.04	
						.0010	.03	29	.01	
300	4.9	6.1	78.9	10.3		0.0344	10.11	2568	1.06	
						.0010	.05	50	.01	
300	0.7	0.7	8.1	1.2		0.0403	9.84	2869	1.05	
						.0011	.10	55	.01	
Total	7.8	11.2	148	16.8		0.0332	10.06	2130	1.05	0.2
						.0010	.04	41	.01	
A-C3(VC) (1.6 g)										
15	1.2	3.6	36.8	2.8		0.0302	9.76	546	0.99	
						.0010	.03	5	.01	
300	3.1	5.5	108	5.6		0.0316	9.88	353	0.98	
						.0010	.02	3	.01	
300	3.7	0.5	6.1	BL		0.0481	9.62	427		
						.0023	.25	5		
Total	8.0	9.6	151	8.4		0.0314	9.81	403	0.98	0.4
						.0010	.04	4	.01	
A-C4(VC)(723.5 mg)										
15	0.6	12.5	155	8.1		0.0294	9.80	357	0.99	
						.0010	.06	7	.01	
300	1.5	9.8	125	7.9		0.0300	10.00	401	1.00	
						.0010	.04	8	.01	
300	BL	BL	8.5	BL				409		
								8		
Total	2.1	22.3	289	16.0		0.0297	9.89	378	1.00	0.2
						.0010	.05	7	.01	
A-C5 (VC)(659.1 mg)										
15	0.2	0.6	7.2	ND		0.0483	10.27	563		
						.0021	.08	10		
300	1.2	1.8	22.2	ND		0.0370	10.01	310		
						.0021	.18	6		
300	BL	BL	3.7	ND				383		
								4		
Total	1.4	2.4	33.1			0.0403	10.08	373		0.1
						.0021	.15	7		

Table 1 (*continued*)

No of strokes(VC) Or °C(P)	^{4}He (10^{-6})	^{22}Ne (10^{-10})	^{36}Ar (10^{-10})	^{132}Xe (10^{-12})	^{3}He/^{4}He (R/R_a)	^{21}Ne/^{22}Ne	^{20}Ne/^{22}Ne	^{40}Ar/^{36}Ar	^{129}Xe/^{132}Xe	^{4}He/^{21}Ne$_{corr}$[a] (10^7)
A-C6(VC)(1.6 g)										
15	0.9	ND	12.6	1.1				1575 15	1.04 .02	
300	17.3	ND	9.6	2.0				3728 36	1.01 .01	
300	7.6	ND	2.2					790 7		
Total	25.8		24.4	3.1				2347 22	1.02 .02	

Unit for abundance is cm^3 STP/g. Errors in concentrations are ±10%. Errors in isotopic ratios are at 95% confidence level. ^{38}Ar/^{36}Ar ratios in the samples are atmospheric within uncertainties.

The mineral name is indicated by letters C(Carbonate), A(Apatite) and M(Magnetite) with a hyper notation after sample name. Numeric after mineral name indicates different sample, while A, B indicates two aliquots. P, VC in parentheses indicates pyrolysis and vacuum crushing respectively.

BL: Blank level. ND: not determined.

  [a] The elemental ratio ^{4}He/^{21}Ne$_{corr}$ has been obtained by correcting for trapped (Air) Ne.

For VC, about a gram of sample was loaded in a stainless steel crusher with a magnetic piston and baked overnight under vacuum at 150 °C. Mantle gases from inclusions may be released during early crushing steps as observed for komatites (Richard et al., 1996). Contrarily, more atmospheric composition has been observed in the initial crush extraction of oceanic basalts and ultramafic xenoliths (Jambon et al., 1985; Sarda et al., 1988; Buikin et al., 2005). Since stepwise crushing helps in better decoupling of magmatic gases from other components present, sample gas was extracted by sequential crushing with a piston activated by an external solenoid. A sequence of three steps of 15, 300 and 300 strokes for carbonates, and 15, 500 and 500 strokes for the apatite and magnetites were followed in order to investigate whether gas composition changed with progressive crushing.

After extraction, the noble gas mixture was purified and separated into individual noble gases using standard procedures (Murty, 1997). He and Ne were separated from the other noble gases using a charcoal trap held at liquid nitrogen temperature to trap the heavier noble gases. The gases were purified using Ti–Zr/Ti getters. A glass extraction system was used for P and a metal system for VC.

Blanks were routinely performed in identical fashion to the sample steps for VC and P (and combustion). Blank compositions were almost atmospheric for all the noble gases. Typical blank concentrations (in 10^{-12} cc STP) for VC are 20(^{4}He), 4.4(^{20}Ne), 0.8(^{36}Ar), 1(^{84}Kr) and 0.3(^{132}Xe), and for P at 1800 °C are 600(^{4}He), 230 (^{20}Ne), 2.2(^{36}Ar), 0.6(^{84}Kr) and 0.1(^{132}Xe). Blank concentrations for ^{4}He are negligible. For all other noble gases except Ne, for which it can be as high as 25% (during P in the glass line) blank contribution does not normally exceed 10% of sample gas.

The isotopic compositions and the elemental abundances for the gases were determined using a VG 1200 mass spectrometer with a resolution of ∼170. Since this does not allow resolution of ^{3}He and the molecular ions of hydrogen (H$_3^+$+HD$^+$), it is necessary to correct for (H$_3^+$+HD$^+$) contribution at mass 3. This is done by measuring the peak at mass 2 (H$_2^+$) and by using a pre-determined (H$_3^+$+HD$^+$)/H$_2^+$ ratio of (4.6± 0.5)×10^{-4} (using pure H$_2$). In the present measurements the interference at mass 3 reached a maximum of ∼20% (for the final crushing step of SV-C1). In some cases, although ^{3}He might have been present, it was difficult to detect it because of the tailing effect of a large ^{4}He peak. Contributions from H$_2^{18}$O$^+$ and ^{40}Ar^{++} at mass 20 and ^{12}C^{16}O$_2^{++}$ at mass 22 can lead to interference effects for Ne isotopes. To minimise mass interference from these species, a liquid nitrogen trap is constantly maintained on the SSM (stainless-steel-mesh) finger open to the mass spectrometer during He–Ne analyses. The Ne data is routinely corrected for these background contributions from the measured peak heights of the masses 18, 40 and 44 and the ^{18}O/^{16}O (normal isotopic ratios), and the abundance ratios of 40^{++}/40$^+$ and 44^{++}/44$^+$ that are periodically determined for the operating conditions of the mass spectrometer. The typical values of 40^{++}/40$^+$ and 44^{++}/44$^+$ are 0.06(±10%) and 0.01(±10%) respectively for the range of ^{40}Ar and CO$_2$ partial pressures observed during sample runs. The mass spectrometer is calibrated for sensitivity and mass discrimination with known amount of air and an artificial He standard. The final

data reported here has been corrected for blanks, background and instrument mass discrimination, and the errors propagated.

The noble gas concentrations and isotopic ratios are listed in Table 1. No systematic difference in concentrations is observed among the different phases. Kr has not been measured for isotopic composition. For Xe, the isotopic composition of only major isotopes could be determined, but here we only report and discuss $^{129}Xe/^{132}Xe$.

4. Results

4.1. Noble gas release pattern

Except for the apatites from Sung Valley (SV-A1 and SV-A2), all other samples were analysed by VC. In the present study, the second VC step was the main extraction step, while the third step ensured complete release of gases from the samples.

During P of SV-A2(P), He and Ne are released at 600–950 °C. About 90% of ^{40}Ar is also released between 600–950 °C. ^{132}Xe and ^{84}Kr are below the detectable limit of the instrument. For SV-A1, where the crushed powder had been analysed by pyrolysis(P′) for He and Ne, most of the He was released at 400 °C and 1200 °C, while nucleogenic Ne, as indicated from isotopic composition, is released at 1400 °C. From earlier studies in apatites it has been seen that trapped Ne from inclusions is released at 600–1400 °C (corresponding to their temperature of decrepitation) while the nucleogenic Ne is released between 1450–1600 °C (Matsumoto et al., 1997). Thus in the present case it is likely that most of the Ne and Ar have been released from the inclusions for SV-A2, although some radiogenic contribution for ^4He cannot be ruled out. P′ of SV-A1 indicates that a part of the trapped Ne may reside in the matrix or small vesicles that survived crushing.

4.2. Light noble gases (Ne and He)

The ^{22}Ne concentration (10^{-10} cm^3 STP/g) for Sung Valley minerals ranges between 0.4–6.2 while for Ambadongar it ranges between 2.4–22.3. The ^{22}Ne concentration during P of the apatites are 117.2 for SV-A1(P′) and 503 for SV-A2 (P). The $^{20}Ne/^{22}Ne$ of up to 12.08 ± 0.29 are measured for the carbonates from Sung Valley but only up to 10.27 ± 0.39 for the magnetites. For Ambadongar, the $^{20}Ne/^{22}Ne$ ratios are comparable in both calcitic (up to 10.19 ± 0.08) and ferro carbonatites (up to 10.27 ± 0.08). For Sung Valley minerals, $^{21}Ne/^{22}Ne$ ratios vary between 0.0309 ± 0.0010 to

0.0543 ± 0.0027 in the carbonates while it is higher for the magnetites (0.0387 ± 0.0013 to 0.0657 ± 0.0048). For Ambadongar, the $^{21}Ne/^{22}Ne$ ratios vary between air and 0.0544 ± 0.0021 and are comparable in calcitic and ferro carbonates.

For He, the measured $^4He(10^{-6}$ cm^3 STP/g) concentration lies between 4.1–81.3 for Sung Valley and between 1.4–25.8 for Ambadongar. $^3He/^4He$ ratios range from 6.95 ± 0.61 R_A to 9.01 ± 0.85 R_A for the Sung Valley magnetites and from 1.04 ± 0.48 R_A to 3.95 ± 0.35 R_A for the carbonates.

4.2.1. In-situ contribution?

In order to ensure minimal cosmogenic He and Ne contribution to the samples, they have been collected from quarries and road cuts so that the locations remained several metres below the top surface of the exposure after emplacement. At such depth cosmogenic neutron flux is very small (Lal, 1987) and the possibility of any ^3He in the samples to be the result of cosmogenic/nucleogenic production can be ruled out. However, contribution from muons is possible if Li is present (Kurz, 1986). So far, no Li rich minerals like spodumene have been reported from Sung Valley carbonatites. Li data is not available for these carbonatites. But using the Li/K ratios observed in Kola carbonatites (Tolstikhin et al., 2002) and the measured K content, we estimate a Li content of < 0.3 ppm, and calculate a maximum muogenic ^3He production of $\approx 3 \times 10^{-12}$ cm^3 STP/g (from both muogenic slow neutrons and negative muons, Kurz, 1986; Lal, 1987) assuming an altitude of < 1000 m and exposure since its emplacement ($\approx$ 100 Ma). This makes up only a few percent of ^3He in the samples and cannot significantly affect the trapped $^3He/^4He$ ratios of the samples.

From earlier studies on carbonatites from Kola by Tolstikhin et al. (2002) it was seen that *in-situ* radiogenic ^4He is released during VC extractions. With prolonged crushing, radiogenic or cosmogenic He diffuses from the matrix even at crushing temperature from newly created fractures (Yokochi et al., 2005). It is interesting to note here that the $^3He/^4He$ of the samples do not evolve with progressive crushing contrary to previous observations from Kola carbonatites (Tolstikhin et al., 2002). This indicates that the measured He isotopic ratios are representative of the signatures trapped at the time of crystallization.

In-situ ^{21}Ne release by VC is unlikely to be significant for both Sung Valley and Ambadongar (except apatite) due to their low emplacement ages. For apatite, contributions from *in-situ* ^{22}Ne produced by the reaction $^{19}F(\alpha,n\beta^+)^{22}Ne$ is also possible and is

reflected in the low $^{20}Ne/^{22}Ne$ ratios of 4.71 ± 0.21(SV-A1) and 8.75 ± 0.11(SV-A2). In Fig. 2, from the plot of $^{22}Ne/^{20}Ne$ vs. $^{21}Ne/^{20}Ne$ for SV-A1 identification of excess ^{21}Ne and ^{22}Ne is straightforward. In Fig. 2 the slope of the trend is dominantly defined by the nucleogenic $^{22}Ne/^{21}Ne$. From the slope (14.8) and using Hünemohr's equation (Hünemohr, 1989) we calculate O/F of ≈17. This falls within the expected range of O/F for apatite (Sasada et al., 1997). Nucleogenic $^{21}Ne/^{22}Ne$ produced in lithospheric mantle or crust would translate into grossly different O/F ratios of ~750 (crust) and $\sim28,000$ (mantle) (Leya and Wieler, 1999). However, although the calculated crustal ratio of O/F ~110 from nucleogenic $^{21}Ne/^{22}Ne$ is lower than the average crustal O/F value (Kennedy et al., 1990), it is still about six times higher than what we see in the apatite. Thus, the apatite is largely dominated by nucleogenic Ne. The high $^{22}Ne/^{20}Ne$ (up to 0.1728 ± 0.0093) and $^{21}Ne/^{20}Ne$ (up to 0.0094 ± 0.0008) for SV-A1 from VC fall on the same trend as P′ in Fig. 2, and also represent in-situ contribution.

4.3. Heavy noble gases (Ar and Xe)

The ^{36}Ar(10^{-10} cm^3/g) concentration varies between 7.7 and 25.3 for Sung Valley and between 24.4 and 289 for Ambadongar. The $^{40}Ar/^{36}Ar$ ratios for Sung Valley show very little variation among the three carbonates SV-C3 (3434 ± 33), SV-C1 (4457 ± 41) and SV-C2 (3082 ± 32) and are similar to the apatite SV-A1
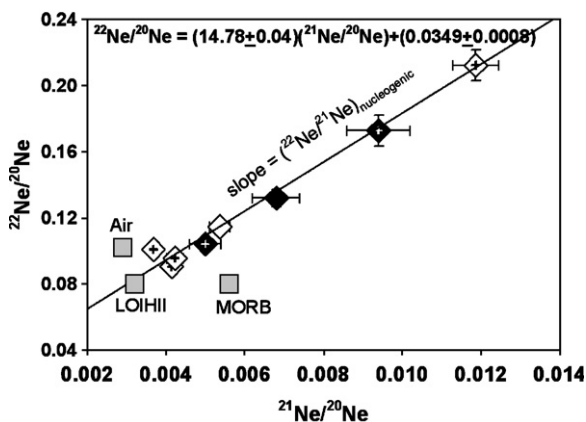
Fig. 2. Plot of $^{22}Ne/^{20}Ne$ vs. $^{21}Ne/^{20}Ne$ for Sung Valley apatite (SV-A1) for P (white symbols) and VC (black symbols). Crossed symbols represent individual crushing steps while filled ones indicate totals. The trend clearly represents addition of nucleogenic $^{22}Ne/^{21}Ne$ represented by the slope of the trend (14.8) to trapped gases. Excesses during VC also fall on the trend indicating contribution of nucleogenic Ne during crushing. The Air, MORB and LOIHII endmembers are also plotted (Moreira et al., 1998; Trieloff et al., 2000).

(3040 ± 24). However, SV-C4 (604 ± 6) and SV-C5 (645 ± 6) have lower ratios which we attribute to atmospheric contamination. Since the contaminant is not removed by baking at 150°C it may be present in microfractures introduced during sampling or sample preparation (Ballentine and Barfod, 2000). The $^{40}Ar/^{36}Ar$ of 1591 ± 14(SV-M3), 1743 ± 28(SV-M1A) and 1386 ± 13(SV-M1B) in the Sung Valley magnetites are lower than their carbonates. Ambadongar ferrocarbonates (A-C3, A-C4 and A-C5) have atmospheric $^{40}Ar/^{36}Ar$ but they are higher for A-C1 (4030 ± 78), A-C2 (2130 ± 41) and A-C6 (2347 ± 22). The K content in the samples is too low (4.6–21.5 ppm) to significantly change the $^{40}Ar/^{36}Ar$ by radiogenic ^{40}Ar ingrowth. Even for SV-C1 with the highest K content of 21.5 ppm, the radiogenic ^{40}Ar produced can only account for 0.02% of the measured ^{40}Ar.

The ^{132}Xe(10^{-12} cm^3/g) concentrations vary between 3.5 and 11.3 for Sung Valley and between 3.1 and 21.9 for Ambadongar carbonates. There was no measurable Xe in the magnetites and apatites. The $^{129}Xe/^{132}Xe$ are up to 1.05 ± 0.01 for Sung Valley and 1.06 ± 0.01 for Ambadongar indicating presence of trapped mantle Xe. Excess ^{129}Xe produced by neutron capture by ^{128}Te, (Bernatowicz et al., 1993) can be ignored for carbonatites as no Te minerals have been reported. The atmospheric $^{40}Ar/^{36}Ar$ of the ferrocarbonatites and SV-C5 is also manifested in low atmospheric $^{129}Xe/^{132}Xe$.

5. Discussion

5.1. Trapped MORB and crustal noble gases: evidence from He–Ne

For the Sung Valley carbonates, plots of $^{20}Ne/^{22}Ne$ (Fig. 3A) and $^{21}Ne/^{22}Ne$ (Fig. 3B) versus $1/^{22}Ne$ show good correlation, indicating mixing between atmospheric and mantle Ne. From these plots, the mantle $^{21}Ne/^{22}Ne\geq0.050$ is close to that typical for MORBs (Moreira et al., 1998). In a Ne three isotope plot (Fig. 4) the Sung Valley carbonates plot on the trend defined by mixing between air and MORB source. This rules out any significant crustal/nucleogenic ^{21}Ne contribution in these carbonates. The MORB Ne isotopic signature is also present in the Sung Valley apatite (SV-A1) where the P′ at 1200 °C yields $^{20}Ne/^{22}Ne=11.06\pm0.26$ and $^{21}Ne/^{22}Ne=0.0458\pm0.0009$. These values are higher than the plume source. Corrected for air using the $^{20}Ne/^{22}Ne$ ratio the source $^{21}Ne/^{22}Ne$ of apatite is 0.0647 ± 0.0073 typically of MORB Ne (Fig. 4).
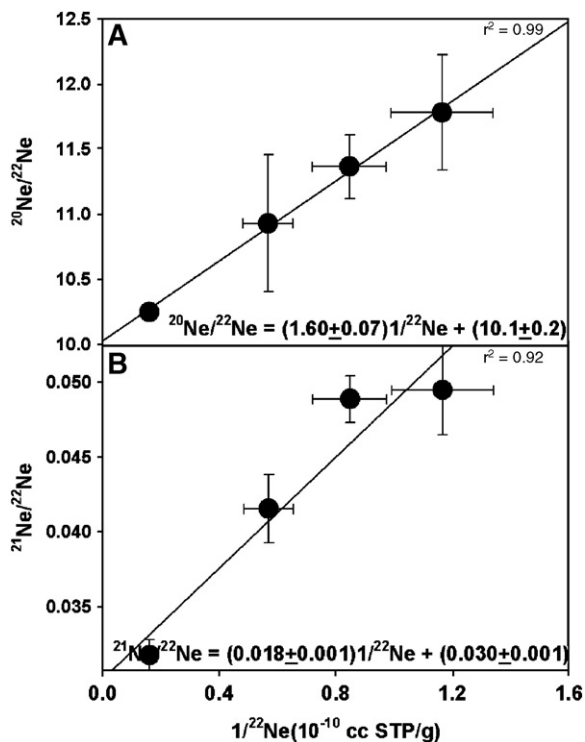
Fig. 3. A)Plot of $1/^{22}Ne$ vs. $^{20}Ne/^{22}Ne$ suggests two component mixing between air and mantle gases in Sung Valley carbonates. B) Intercept from the plot $1/^{22}Ne$ vs. $^{21}Ne/^{22}Ne$ suggests addition of MORB like mantle gases ($^{21}Ne/^{22}Ne \geq 0.05$) to air component. For discussion see text.

The $^{3}He/^{4}He$ up to 9.01 ± 0.85 R_A of Sung Valley magnetites fall within the MORB range. However, the lower $^{3}He/^{4}He$ ratios in the coexisting carbonates require the presence of an additional component.

Although the magnetites are enriched in nucleogenic Ne compared to the carbonates, their MORB-like $^{3}He/^{4}He$ appear to be unaffected. It is difficult to attribute the high $^{21}Ne/^{22}Ne$ signature to either subducted crustal Ne or lithospheric mantle that has undergone enrichment in lithophile elements resulting in high U/Ne ratio (Honda et al., 2003), since such a signature should be recorded by carbonates also. For the carbonates, while the Ne isotopic signatures are MORB like, the $^{3}He/^{4}He$ ratios (upto 3.95 ± 0.35 R_A) are more radiogenic and indicate strong crustal contributions.

For Ambadongar, the high $^{21}Ne/^{22}Ne$ ratios could reflect crustal Ne in the lithospheric mantle. In fact, higher $\delta^{13}C$ than normal mantle had been attributed to ^{13}C enriched recycled subducted crust from the subcontinental lithosphere for Ambadongar carbonatites (Ray et al., 2000). Involvement of continental lithosphere in carbonatite magmatism has been suggested earlier in Kola and East Africa from Nd and Sr

measurements (Bell and Blekinshop, 1989; Kramm and Kogardo, 1994). Recently, noble gas composition in polycrystalline diamonds from Jwaneng kimberlite indicate that crustal noble gases can be introduced into the sub-continental lithospheric mantle during ancient subduction (Honda et al., 2003). From Fig. 4, MORB-like Ne in Ambadongar is largely dominated by atmospheric and lithospheric mantle components. Contribution of both MORB and continental lithosphere for Ambadongar carbonatites had been observed from Nd, Pb and Sr isotopes (Simonetti et al., 1998).

5.2. He/Ne fractionation (Sung Valley)

It is not possible to account for the low $^{3}He/^{4}He$ of the carbonates to fractionation due to loss of He as $^{4}He/^{21}Ne_{corr}$ (obtained by correcting ^{21}Ne for air contribution assuming all measured ^{20}Ne to be atmospheric; see Table 1) is identical for the carbonates and magnetites from same hand specimen. Differential isotopic evolution of He and Ne attributed to late stage volatile loss has been observed in North Chile Ridge basalts (Niedermann and Bach, 1998). A reduced concentration of He and Ne relative to U and Th in the degassed melt, resulted in lowering of $^{3}He/^{4}He$ and an increase of $^{21}Ne/^{22}Ne$ over time, although the Ne isotopic values altered more readily than that of He.
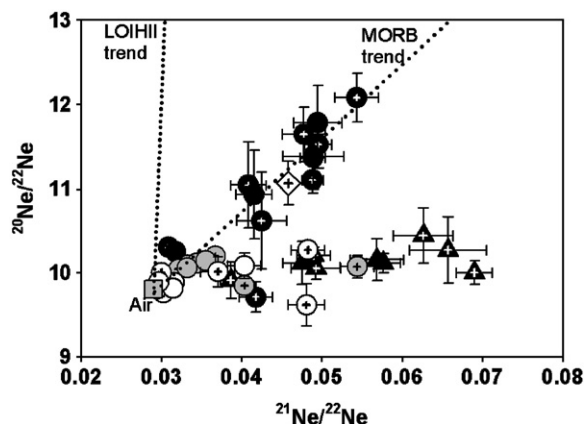

Fig. 4. Ne 3-isotope plot for Sung Valley carbonates (black circle) and magnetites (black triangles), and Ambadongar calcitic carbonatites (grey circles) and ferrocarbonaties (white circles). Crossed symbols represent individual crushing steps while filled ones indicate totals. The crossed diamond represents the 1200 °C heating step for Sung Valley apatite. LOIHII and MORB trends as in Trieloff et al. (2000) are indicated. The plot clearly indicates presence of MORB volatiles for both Sung Valley and Ambadongar, but Ambadongar is dominated by a larger atmospheric contribution. For both Ambadongar and the Sung Valley magnetites, in addition, an enriched $^{21}Ne/^{22}Ne$ component attributed to subducted crustal component from the lithosphere is observed. For discussion see text.

However, in the present study this fails to account for the crustal signatures of He in the carbonates without affecting the MORB-like Ne.

The solubility of noble gases in carbonatitic melts is unknown. However, assuming a similar behaviour to silicate melts, a plausible scenario could involve progressive increase of the relative He/Ne ratio between the degassed residual melt (derived from MORB source) and the vapour phase. Subsequent addition of the crustal noble gases during assimilation of the lithospheric mantle component would affect He to a greater degree in the carbonates and the Ne isotopic composition of the late crystallising magnetites as the relative He/Ne ratio of the residual melt increases as degassing proceeds. That the carbonates are barely influenced by crustal Ne while their He composition shows crustal signatures suggests that the initial Ne/He of the magma was considerably higher relative to the crustal component being assimilated from the lithosphere. From Pb, Sr and Nd isotopic systematics, contribution of sub-continental lithosphere had been speculated (Veena et al., 1998). Entrainment of oceanic crust from subcontinental lithospheric mantle has been suggested based on enriched ^{13}C signatures in agreement with our observations from noble gases (Ray et al., 1999).

5.3. Ne–Ar relationship

In Fig. 5A, we plot the $^{20}Ne/^{22}Ne$ vs. $^{40}Ar/^{36}Ar$ for both the regions. The $^{40}Ar/^{36}Ar$ of the Sung Valley carbonates and magnetites are positively correlated with $^{20}Ne/^{22}Ne$ resulting from mixing between a mantle and atmospheric noble gases. SV-C4 and SV-C5 that show presence of atmospheric contaminant ($^{40}Ar/^{36}Ar < 1000$) have not been plotted. Correlated trends are commonly observed in various mantle samples like deformed xenoliths and MORB glasses (Farley et al., 1994; Trieloff et al., 2000). In such a plot mixing is represented by hyperbolae. (Fig. 5B). In Fig. 5B, mixing lines for air–MORB mixtures are shown for R $[(^{22}Ne/^{36}Ar)_{air}/(^{22}Ne/^{36}Ar)_{MORB}] = 0.06$ and 0.6, following estimation by Farley and Poreda (1993). However, since atmospheric contamination may be a late stage process probably affecting samples after Ne/Ar fractionation in the course of magmatic evolution, mixing hyperbolae curvatures must be taken from individual samples (Buikin et al., 2005). In Fig. 5B, the best-fit mixing hyperbolae for the individual Sung Valley samples define curvatures of $R = 0.06$ to 0.6. In Fig. 5C ($^{21}Ne/^{22}Ne$ vs. $^{40}Ar/^{36}Ar$) it is clearly seen that the carbonates can be explained by air–MORB mixing, but the magnetites have excess ^{21}Ne
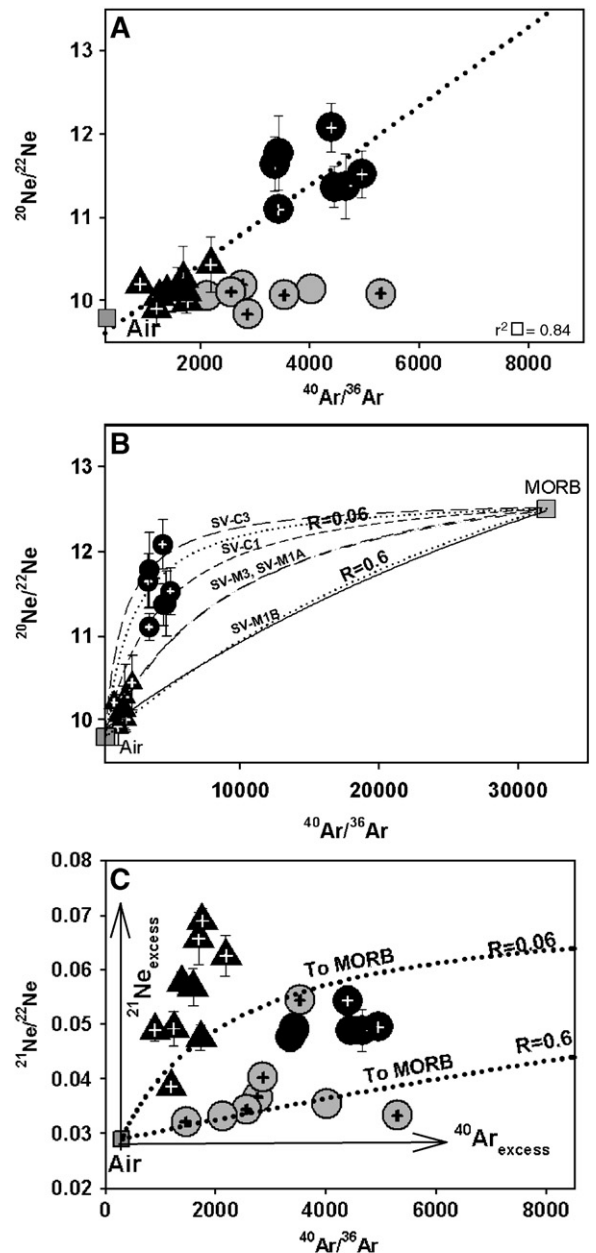

Fig. 5. A) Plot of $^{40}Ar/^{36}Ar$ vs. $^{20}Ne/^{22}Ne$ for Sung Valley and Ambadongar. Symbols as in Fig. 4. Correlated trend for Sung Valley indicates mixing between MORB and Air. For Ambadongar, similar correlation is not observed B) Best fit air–MORB mixing hyperbolae for individual Sung Valley carbonates and magnetites (indicated against corresponding trends). All samples can be explained by expected air–MORB mixing with $R = 0.06$ to 0.6 (dotted) as estimated by Farley and Poreda (1993) where $R = (^{22}Ne/^{36}Ar)_{air}/(^{22}Ne/^{36}Ar)_{MORB}$. C) Plot of $^{40}Ar/^{36}Ar$ vs. $^{21}Ne/^{22}Ne$ that clearly shows excess ^{21}Ne for the Sung Valley magnetites attributed to subducted crustal component from the lithosphere. For Ambadongar, no correlated enrichment is observed for ^{40}Ar and ^{21}Ne indicating different or more than one sources. All the carbonates can be reasonably explained by air–MORB mixing.

that can be attributed to subducted crustal component from the lithosphere as discussed earlier. It is difficult to discern if the lower $^{40}Ar/^{36}Ar$ are solely due to contamination, or if they reflect subduction of air-like noble gases to the mantle (Mohapatra and Murty, 2000; Matsumoto et al., 2001; Yamamoto et al., 2004). Coupled analysis of Ar with isotopic tracers like N, where $\delta^{15}N$ is distinct for subduction will provide better constrains (Mohapatra and Murty, 2000).

For Ambadongar, in Fig. 5A, no correlation is observed between $^{40}Ar/^{36}Ar$ and $^{20}Ne/^{22}Ne$ ratios where the later is largely dominated by atmospheric gases. Like the $^{21}Ne/^{22}Ne$ signatures, the $^{40}Ar/^{36}Ar$ ratios may also be attributed to contribution from a crustal component from the lithospheric mantle. But no straightforward correlation is observed between excess (above atmospheric) ^{40}Ar and ^{21}Ne in the samples as seen in Fig. 5C indicating possibly different or more than one sources contributing to the excesses.

5.4. Ar–Xe relationship

Fig. 6 is a plot of $^{129}Xe/^{132}Xe$ vs. $^{40}Ar/^{36}Ar$ for MORBs from different locations, and Brazilian and Canadian carbonatites. They plot on distinct trends of R
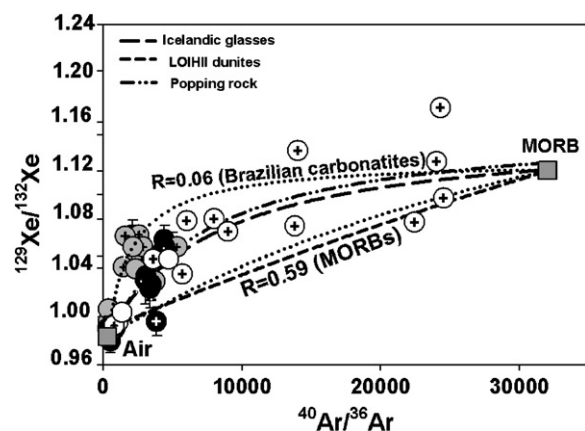

Fig. 6. Plot of $^{40}Ar/^{36}Ar$ vs. $^{129}Xe/^{132}Xe$ for Sung Valley and Ambadongar carbonates. Symbols as in Fig. 4. Mixing trends for $R=0.06$ (Brazilian carbonatites) and $R=0.6$ (MORBs) where $R = (^{132}Xe/^{36}Ar)_{air}/(^{132}Xe/^{36}Ar)_{mantle}$ is shown (Sasada et al., 1997). Best fit mixing hyperbola for Icelandic, LOIHII basalts and MORB popping rock ($2\pi D43$) have been plotted using data from Moreira et al. (1998), Trieloff et al. (2000). Data points for $2\pi D43$ from Moreira et al. (1998) are also shown (white circles; crossed symbols represent individual crushing steps). Clearly, no unique trend can be ascribed to MORB or plume samples. High $^{129}Xe/^{132}Xe$ ratios accompanying lower $^{40}Ar/^{36}Ar$ ratios observed for carbonatites is also seen for MORB popping rock and cannot be considered unique to the carbonatitic mantle source. For discussion see text.

$[(^{132}Xe/^{36}Ar)_{air}/(^{132}Xe/^{36}Ar)_{mantle}]$ (Sasada et al., 1997). The carbonatites plot on the trend defined by $R=0.06$ and are characterised by high $^{129}Xe/^{132}Xe$ accompanied by lower $^{40}Ar/^{36}Ar$ that lie in the range of mantle source that is less degassed than the MORB (Sasada et al., 1997). Neither Sung Valley nor Ambadongar carbonates, plot on the trend defining air–MORB mixing but they plot close to the trend defined by $R=0.06$ (Fig. 6). However, the hyperbolae curvatures maybe sample specific explaining some scatter of the data observed.

In Fig. 6, best fit mixing hyperbola have been plotted for Loihi, Icelandic and MORB ($2\pi D43$ — popping rock) basalts using data from Moreira et al. (1998) and Trieloff et al. (2000). It is unlikely that there is any unique hyperbola with unique elemental ratios describing all MORB samples. For example, the Loihi basalts characterising the plume source plot on the MORB trend defined by Sasada et al., 1997. The MORB $2\pi D43$ defines a trend similar to the Icelandic basalts but distinct from $R=0.6$. Also, there are at least five $2\pi D43$ data with high $^{129}Xe/^{132}Xe$ ratios and quite low $^{40}Ar/^{36}Ar$ ratios. It is therefore obvious that the hyperbola curvatures depend on the specific elemental ratios of mantle gases and the atmosphere derived component both of which undergo elemental fractionation. Therefore, for all practical purposes, Xe–Ar relationship maybe considered to indicate dominantly mixing between Air and MORB components. It would be necessary to study the Brazilian and Canadian carbonatites, for other noble gases (He and Ne) to further constrain the trapped components, as it might be erroneous to advocate a less degassed mantle component distinct from MORB only based on high $^{129}Xe/^{132}Xe$ accompanied by lower $^{40}Ar/^{36}Ar$ as done by Sasada et al. (1997).

5.5. Late stage hydrothermal activity

The lower $^{40}Ar/^{36}Ar$ ratios for the magnetites can be attributed to their interaction with air saturated hydrothermal fluids and/or meteoric water, which, for most also affected their $^{20}Ne/^{22}Ne$. Evidences of late alteration is also apparent from variation of $\delta^{13}C$ and $\delta^{18}O$ (Ray and Ramesh, 2006). For the ferrocarbonatites of Ambadongar, the low $^{40}Ar/^{36}Ar$ are possibly also related to hydrothermal activity involving large-scale participation of ground water that produced extreme ^{18}O enrichment (Viladkar and Schidlowski, 2000). Although the Ne isotopic ratios of the ferrocarbonatites are not grossly different from the calcitic carbonatites, the atmospheric signatures are more strongly manifested in

their Ar isotopes indicating presence of a fractionated atmospheric contaminant.

5.6. Petrogenetic implications

The noble gas results from this study suggest that Sung Valley carbonatites have contribution from a MORB-like source. It is therefore possible that basalts from Rajmahal and the Ninetyeast Ridge, both of which show depleted upper mantle component and along with Sung Valley constitute a chain of magmatic activity that ensued during the continental break-up and opening of the Indian Ocean (Veena et al., 1998), have the same magma sources. Also, from this study there is indication of contribution of crust, probably subducted into the subcontinental lithospheric mantle. Evidences of late stage alteration is manifested in the late crystallising magnetites by more air-like $^{20}Ne/^{22}Ne$ and $^{40}Ar/^{36}Ar$ ratios that can be attributed to hydrothermal fluids and/ or meteoric water. Noble gases in Ambadongar also show similar trapped components though the MORB signatures are less pronounced. This is possibly due to the shallower level of emplacement of Ambadongar making it more prone to atmospheric contamination.

Both Sung Valley and Ambadongar carbonatites have been attributed to plume origin (Ray et al., 1999, 2000). Absence of a plume-type signature is consistent with derivation in the waning stages of volcanism after entrainment of MORB and assimilation of the crustal component from the overlying lithosphere by the plume head. A similar phenomenon of dilution of the plume component by MORB entrainment in the waning stages of magmatism had been observed from the study of noble gases in the Yellowstone plume basalts from Imnaha formation, Columbia River Basalt (Dodson et al., 1997). That the Sung Valley represent late magmatic pulses of the associated Rajmahal–Bengal–Sylhet flood basalt province is evident from its younger age as compared to the magmatic activity of Sylhet (110±3 to 133±4 Ma; Sarkar et al., 1996), Bengal and Rajmahal (117±2 Ma; Baksi, 1995). In contrast, noble gases in Kola carbonatites are dominated by the plume compo- nent (Marty et al., 1998; Tolstikhin et al., 2002). This can be explained if the Kola carbonatites were generated during the early stages of plume–lithosphere interaction unlike Sung Valley and Ambadongar.

6. Summary and conclusions

Our results clearly show the presence of volatiles from a MORB source and subcontinental lithosphere enriched in crustal noble gases, probably introduced

into the mantle during subduction for Sung Valley. This is variably manifested in the He and Ne isotopic signatures of the carbonates and magnetites analysed. If the relative He/Ne ratios progressively increases between the MORB derived magma and the degassing vapour, subsequent addition of crustal component from lithospheric mantle would be strongly reflected in the Ne isotopic signatures of the late crystallising magnetites and He isotopic ratios of the earlier carbonates. Although the MORB component could be identified from Ne in apatite, it is more dominated by nucleogenic signatures. For Ambadongar, (like for Sung Valley), both MORB and a crustal component (incorporated from the lithospheric mantle) could be identified, though the MORB signatures are far less pronounced owing to their shallow level of emplace- ment and overprinting by atmospheric gases. In both Sung Valley and Ambadongar, late stage hydrothermal activity played a major role in diluting magmatic signatures.

In Sung Valley and Ambadongar, contribution from MORB and lithospheric mantle sources were observed contrary to the Kola carbonatites which was dominated by plume type noble gases. This is possibly because these carbonatites were generated in the waning stages of plume magmatism with considerable entrainment and input from the lithospheric and MORB sources with dilution and replacement of the uprising plume component after it induced melting.

References

Allègre, C.J., Staudacher, T., Sarda, P., Kurz, M., 1983. Constraints on evolution of Earth's mantle from rare gas systematics. Nature 303, 762–766.

Baksi, A.K., 1995. Petrogenesis and timing of volcanism in the Rajmahal flood basalt province, northeastern India. Chem. Geol. 121, 73–90.

Ballentine, C.J., Barfod, D.N., 2000. The origin of air-like noble gases in MORB and OIB. Earth Planet. Sci. Lett. 180, 39–48.

Barker, D.S., 1989. Field relations of carbonatites. In: Bell, K. (Ed.), Carbonatites: Genesis and Evolution. Unwin Hyman Ltd, London, pp. 38–69.

Basu, A.R., Renne, P.R., Das Gupta, D.K., Teichman, F., Poreda, R.J., 1994. Early and late alkali igneous pulses and a high ^{3}He plume origin for the Deccan flood basalts. Science 261, 902–906.

Bell, K., 2002. Probing the mantle: the story from carbonatites. Eos, Transactions, American Geophysical Union, vol. 83, No. 25.

Bell, K., Blekinshop, J., 1987. Archean depleted mantle: evidence from neodymium and strontium initial isotopic ratio of carbonatites. Geochim. Cosmochim. Acta 51, 291–298.

Bell, K., Blekinshop, J., 1989. Neodymium and Sr isotope geochemistry of carbonatites. In: Bell, K. (Ed.), Carbonatites: Genesis and Evolution. Unwin Hyman Ltd, London, pp. 278–300.

Bernatowicz, T., Brannon, J., Brazzle, R., Cowsik, R., Hohenberg, C., Podosek, F., 1993. Precise determination of relative and absolute $\beta\beta$-decay rates of ^{128}Te and 1^{30}Te. Phys. Rev. 47, 1905–1915.

Buikin, A., Trieloff, M., Hopp, J., Althaus, T., Korochantseva, E., Schwarz, W.H., Alther, R., 2005. Noble gas isotopes suggest deep mantle plume source of late Cenozoic mafic alkaline volcanism in Europe. Earth Planet. Sci. Lett. 230, 143–162.

Dodson, A., Kennedy, B.M., DePaolo, D.J., 1997. Helium and neon isotopes in the Imnaha Basalt, Columbia River Basalt Group: evidence for a Yellowstone plume source. Earth Planet. Sci. Lett. 150, 443–451.

Farley, K.A., Poreda, R.J., 1993. Mantle neon and atmospheric contamination. Earth Planet. Sci. Lett. 114, 325–339.

Farley, K.A., Poreda, R.J., Onstott, T.C., 1994. noble Gases in deformed xenoliths from an ocean island: characterization of a metasomatic fluid. In: Matsuda, K. (Ed.), Noble Gas Geochemistry and Cosmochemistry. Terra Scientific Publishing Company, Tokyo, pp. 159–178.

Hogarth, D.D., 1989. Pyrochlore, apatite and amphibole: distinctive minerals in carbonatites. In: Bell, K. (Ed.), Carbonatites: Genesis and Evolution. Unwin Hyman Ltd, London, pp. 105–148.

Honda, M., Phillips, D., Harris, J.W., Yatsevich, I., 2003. Unusual noble gas compositions in polycrystalline diamonds: preliminary results from the Jwaneng kimberlite, Botswana. Chem. Geol. 203, 347–358.

Hûnemohr, H., 1989. Edelgase in U- und Th-reichen Mineralen und die Bestimmung der ^{21}Ne-Dicktarget-Ausbeute der ^{18}O$(\alpha,n)^{21}$Ne-kernreaktion im Bereich 4.0–8.8 MeV. PhD thesis, Johannes Gutenberg-University, Mainz, Germany.

Jambon, A., Weber, H.W., Begemann, F., 1985. Helium and argon from an Atlantic MORB glass: concentration, distribution and isotopic composition. Earth Planet. Sci. Lett. 73, 255–267.

Javoy, M., Pineau, F., Staudacher, T., Cheminee, J.L., Krafft, M., 1989. Mantle volatiles sampled from a continental rift: the 1988 eruption of Oldoinyo Lengai (Tanzania). Terra 1, 324 (abstr.).

Kennedy, B.M., Hiyagon, H., Reynolds, J.H., 1990. Crustal neon: a striking uniformity. Earth Planet. Sci. Lett. 98, 277–286.

Kent, R.W., Storey, M., Saunders, A.D., 1992. Large igneous provinces: site of plume impact or plume incubation? Geology 20, 891–894.

Kramm, U., Kogardo, L.N., 1994. Nd and Sr isotopic signatures of the Khibina and Lovozero agpaitic centres, Kola alkaline province, Russia. Lithos 32, 225–242.

Krishnamurthy, P., 1988. Carbonatites of India. Explor. Res. At. Miner. 1, 81–115.

Kumar, D., Mamallan, R., Dwivedy, K.K., 1996. Carbonatite magmatism in northeast India. J. Southeast Asian Earth Sci. 13, 145–158.

Kumar, A., Dayal, A.M., Padmakumari, V.M., 2003. Kimberlite from Rajmahal magmatic province: Sr–Nd–Pb isotopic evidence for

Kerguelen plume derived magmas. Geophys. Res. Lett. 30. doi:10.1029/2003GL018462.

Kurz, M.D., 1986. In situ production of terrestrial cosmogenic helium and some applications to geochronology. Geochim. Cosmochim. Acta 50, 2855–2862.

Kwon, S.T., Tilton, G.R., Grunenfelder, M.H., 1989. Lead isotope relationships in carbonatites and alkalic complexes: an overview. In: Bell, K. (Ed.), Carbonatites: Genesis and Evolution. Unwin Hyman Ltd., London, pp. 360–387.

Lal, D., 1987. Production of ^{3}He in terrestrial rocks. Chem. Geol. 66, 89–98.

Leya, I., Wieler, R., 1999. Nucleogenic production of Ne isotopes in Earth's crust and upper mantle induced by alpha particles from the decay of U and Th. J. Geophys. Res. 104 (B7), 15439–15450.

Marty, B., Tolstikhin, I., Kamensky, I.L., Nivin, V., Balaganskaya, E., Zimmermann, J.L., 1998. Plume-derived rare gases in 380 Ma carbonatites from the Kola region (Russia) and the argon isotopic composition in the deep mantle. Earth Planet. Sci. Lett. 164, 179–192.

Matsumoto, T., Honda, M., McDougall, I., Yatsevich, I., O'Reilly, S.Y., 1997. Plume-like neon in a metasomatic apatite from the Australian lithospheric mantle. Nature 388, 162–164.

Matsumoto, T., Chen, Y., Matsuda, J., 2001. Concomitant occurrence of primordial and recycled noble gases in the Earth's mantle. Earth Planet. Sci. Lett. 185, 35–47.

Mohapatra, R.K., Murty, S.V.S., 2000. Origin of air like noble gases in oceanic basalts. Geophys. Res. Lett. 27, 1583–1586.

Moreira, M., Kunz, J., Allegre, C.J., 1998. Rare gas systematics in popping rock: isotopic and elemental compositions in the upper mantle. Science 279, 1178–1181.

Murty, S.V.S., 1997. Noble gases and nitrogen in Muong Nong tektites. Meteorit. Planet. Sci. 32, 687–691.

Niedermann, S., Bach, W., 1998. Anomalously nucleogenic neon in north Chile ridge basalt glasses suggesting a previously degassed mantle source. Earth Planet. Sci. Lett. 160, 447–462.

Ray, J.S., Ramesh, R., 2006. Stable carbon and oxygen isotopic compositions of Indian carbonatites. Int. Geol. Rev. 48, 17–45.

Ray, J.S., Ramesh, R., Pande, K., 1999. Carbon isotopes in Kerguelen plume-derived carbonatites: evidence for recycled inorganic carbon. Earth Planet. Sci. Lett. 170, 205–214.

Ray, J.S., Trivedi, J.R., Dayal, A.M., 2000. Strontium isotope systematics of Amba Dongar and Sung Valley carbonatite–alkaline complexes, India: evidence for liquid immiscibility, crustal contamination and long-lived Rb/Sr enriched mantle sources. J. Asian Earth Sci. 18, 585–594.

Richard, D., Marty, B., Chaussidon, M., Arndt, N., 1996. Helium isotopic evidence for a lower mantle component in depleted Archean Komatite. Science 273, 93–95.

Sarda, P., Staudacher, T., Allègre, C.J., 1988. Neon isotopes in submarine basalts. Earth Planet. Sci. Lett. 91, 73–88.

Sarkar, A., Datta, A.K., Poddar, B.C., Bhattacharya, B.K., Kollapuri, V.K., Sanwal, R., 1996. J. Asian Earth Sci. 13, 77–81.

Sasada, T., Hiyagon, H., Bell, K., Ebihara, M., 1997. Mantle derived noble gases in carbonatites. Geochim. Cosmochim. Acta 61, 4219–4228.

Secher, K., Larson, L.M., 1980. Geology and mineralogy of the Sarafartoq carbonatite complex, southern west Greenland. Lithos 13, 199–212.

Simonetti, A., Goldstein, S.L., Schmidberger, S.S., Viladkar, S.G., 1998. Geochemical and Nd, Pb, and Sr isotope data from Deccan alkaline complexes — inferences for mantle sources and plume–lithosphere interaction. J. Petrol. 39, 1847–1864.

Staudacher, T., Sarda, P., Richardson, S.H., Allègre, C.J., Sagna, I., Dmitriev, L.V., 1989. Noble gases in basalt glasses from a Mid-Atlantic Ridge topographic high at 14°N: geodynamic consequences. Earth. Planet. Sci. Lett. 96, 119–133.

Stuart, F.M., Lass-Evans, S., Fitton, J.F., Ellam, R.M., 2003. High ^{3}He/^{4}He ratios in picritic basalts from Baffin Island and the role of a mixed reservoir in mantle plumes. Nature 424, 57–59.

Tolstikhin, I.N., Kamensky, I.L., Marty, B., Nivin, V.A., Vetrin, V.R., Balaganskaya, E.G., Ikorsky, S.V., Gannibal, M.A., Weiss, D., Verhulst, A., Demaiffe, D., 2002. Rare gas isotopes and parent trace elements in ultrabasic–alkaline–carbonatite complexes, Kola Peninsula: identification of lower mantle plume component. Geochim. Cosmochim. Acta 66, 881–901.

Trieloff, M., Kunz, J., Clague, D.A., Harrison, D., Allegre, C.J., 2000. Noble gas systematics of the Reunion mantle plume source and the origin of primordial noble gases in Earth's mantle. Science 288, 1036–1038.

Trieloff, M., Falter, M., Jessberger, E.K., 2003. The distribution of mantle and atmospheric argon in oceanic basalt glasses. Geochim. Cosmochim. Acta 67, 1229–1245.

Veena, K., Pandey, B.K., Krishnamurthy, P., Gupta, J.N., 1998. Sr and Nd isotopic systematics of Sung Valley, Meghalaya, Northeast India: implication for contemporary plume-related mantle source characteristics. J. Petrol. 39, 1975–1984.

Viladkar, S.G., 1981. The carbonatites of Ambadongar, Gujarat, India. Bull. Geol. Soc. Finl. 53, 17–28.

Viladkar, S.G., Schidlowski, M., 2000. Carbon and oxygen isotope geochemistry of the Amba Dongar carbonatite complex, Gujarat, India. Gondwana Res. 3, 415–424.

Yamamoto, J., Kaneoka, I., Nakai, S., Kagi, H., Prikhod'ko, V.S., Arai, S., 2004. Evidence for subduction-related components in the subcontinental mantle from low ^{3}He/^{4}He and ^{40}Ar/^{36}Ar ratio in mantle xenoliths from far eastern Russia. Chem. Geol. 207, 237–259.

Yokochi, R., Marty, B., 2004. A determination of the neon isotopic composition of the deep mantle. Earth Planet. Sci. Lett. 225, 77–88.

Yokochi, R., Marty, B., Pik, R., Burnard, P., 2005. High ^{3}He/^{4}He ratios in peridotite xenoliths from SW Japan revisited: evidence for cosmogenic ^{3}He released by vacuum crushing. Geochem. Geophys. Geosyst. 6. doi:10.1029/2004GC000836.